

# Clinically Relevant and Minimally Invasive Tumor Surveillance of Pediatric Diffuse Midline Gliomas Using Patient-Derived Liquid Biopsy



Eshini Panditharatna<sup>1,2</sup>, Lindsay B. Kilburn<sup>3,4</sup>, Mariam S. Aboian<sup>5</sup>, Madhuri Kambhampati<sup>1</sup>, Heather Gordish-Dressman<sup>1</sup>, Suresh N. Magge<sup>6</sup>, Nalin Gupta<sup>7</sup>, John S. Myseros<sup>6</sup>, Eugene I. Hwang<sup>3,4</sup>, Cassie Kline<sup>8</sup>, John R. Crawford<sup>9</sup>, Katherine E. Warren<sup>10</sup>, Soonmee Cha<sup>11</sup>, Winnie S. Liang<sup>12</sup>, Michael E. Berens<sup>12</sup>, Roger J. Packer<sup>4</sup>, Adam C. Resnick<sup>13</sup>, Michael Prados<sup>14</sup>, Sabine Mueller<sup>14</sup>, and Javad Nazarian<sup>1,3,4,15</sup>

## Abstract

**Purpose:** Pediatric diffuse midline glioma (DMG) are highly malignant tumors with poor clinical outcomes. Over 70% of patients with DMG harbor the histone 3 p.K27M (H3K27M) mutation, which correlates with a poorer clinical outcome, and is also used as a criterion for enrollment in clinical trials. Because complete surgical resection of DMG is not an option, biopsy at presentation is feasible, but rebiopsy at time of progression is rare. While imaging and clinical-based disease monitoring is the standard of care, molecular-based longitudinal characterization of these tumors is almost nonexistent. To overcome these hurdles, we examined whether liquid biopsy allows measurement of disease response to precision therapy.

**Experimental Design:** We established a sensitive and specific methodology that detects major driver mutations associated with pediatric DMGs using droplet digital PCR ( $n = 48$  subjects,  $n = 110$  specimens). Quantification of circulating

tumor DNA (ctDNA) for H3K27M was used for longitudinal assessment of disease response compared with centrally reviewed MRI data.

**Results:** H3K27M was identified in cerebrospinal fluid (CSF) and plasma in 88% of patients with DMG, with CSF being the most enriched for ctDNA. We demonstrated the feasibility of multiplexing for detection of H3K27M, and additional driver mutations in patient's tumor and matched CSF, maximizing the utility of a single source of liquid biomedicine. A significant decrease in H3K27M plasma ctDNA agreed with MRI assessment of tumor response to radiotherapy in 83% (10/12) of patients.

**Conclusions:** Our liquid biopsy approach provides a molecularly based tool for tumor characterization, and is the first to indicate clinical utility of ctDNA for longitudinal surveillance of DMGs. *Clin Cancer Res*; 24(23); 5850–9. ©2018 AACR.

## Introduction

High-grade gliomas in children are rare, accounting for about 20% of all pediatric central nervous system (CNS) cancers. Nevertheless, pediatric brain cancers are the leading cause of cancer-related mortality in children under 14 years of age (1). Among these, malignant tumors arising in midline brain structures (e.g., pons, thalamus, spinal cord) have one of the worst outcomes

(2, 3). Children with diffuse midline glioma (DMG), including those with diffuse intrinsic pontine glioma (DIPG), have a median survival of only 12 months. DMGs often harbor mutations in genes encoding canonical histones H3.1 (*HIST1H3B/C*), H3.2 (*HIST2H3C*), and noncanonical histone H3.3 (*H3F3A*) variants (2–5). The presence of these mutations often confers a poorer outcome as compared with tumors without these alterations (2). On the basis of distinct genetic features and clinical behavior,

<sup>1</sup>Research Center for Genetic Medicine, Children's National Health System, Washington, D.C. <sup>2</sup>Institute for Biomedical Sciences, George Washington University School of Medicine and Health Sciences, Washington, D.C. <sup>3</sup>Center for Cancer and Blood Disorders, Children's National Health System, Washington D.C. <sup>4</sup>Brain Tumor Institute, Children's National Health System, Washington, D.C. <sup>5</sup>Departments of Neurology, Pediatrics and Neurosurgery, University of California, San Francisco School of Medicine, San Francisco, California. <sup>6</sup>Division of Neurosurgery, Children's National Health System, Washington, D.C. <sup>7</sup>Department of Neurological Surgery and Pediatrics, University of California San Francisco, San Francisco, California. <sup>8</sup>Pediatric Hematology-Oncology and Neurology, UCSF Benioff Children's Hospital, San Francisco, California. <sup>9</sup>Department of Neurosciences, UC San Diego School of Medicine, La Jolla, California. <sup>10</sup>National Cancer Institute, NIH, Bethesda, Maryland. <sup>11</sup>Department of Radiology, University of California, San Francisco School of Medicine, San Francisco, California. <sup>12</sup>Translational Genomics Research Institute, Phoenix, Arizona. <sup>13</sup>Center for Data-Driven Discovery, Children's Hospital of Philadelphia, Philadelphia, Pennsylvania. <sup>14</sup>Departments of Neurology, Pediatrics and

Neurosurgery, University of California, San Francisco School of Medicine, San Francisco, California. <sup>15</sup>Department of Genomics and Precision Medicine, George Washington University School of Medicine and Health Sciences, Washington, D.C.

**Note:** Supplementary data for this article are available at Clinical Cancer Research Online (<http://clincancerres.aacrjournals.org/>).

S. Mueller and J. Nazarian are the co-senior authors of this article.

**Corresponding Author:** Javad Nazarian, Genomics and Precision Medicine, Children's National Health System, Center for Genetic Medicine Research, George Washington University, School of Medicine and Health Sciences 111 Michigan Ave., NW, Washington DC 20010. Phone: 202-476-6022; Fax: 202-476-6014; E-mail: jnazarian@childrensnational.org

**doi:** 10.1158/1078-0432.CCR-18-1345

©2018 American Association for Cancer Research.

### Translational Relevance

Performing stereotactic biopsies in patients with diffuse midline glioma (DMG), including diffuse intrinsic pontine glioma (DIPG), has become more widely accepted. However, due to risks, costs, and clinical regulations associated with the procedure, rebiopsy is rarely performed at disease progression. Inability to accurately assess disease response and molecular changes are major hurdles for developing successful therapeutic interventions. Liquid biopsy is a minimally invasive method for detecting tumor-associated circulating DNA (ctDNA). We investigated the feasibility of using liquid biopsy for detecting primary driver mutations in patients with DMG. We established a molecular-based tool to detect rare mutant alleles, with the objective of complementing diagnosis, and clinical monitoring. Each patient's response to precision therapies was successfully monitored in real-time using ctDNA as a surrogate biomarker of tumor response. This is the first evidence of clinical translational utility to measure ctDNA for longitudinal tumor surveillance in this devastating pediatric disease.

these tumors were recently reclassified by the World Health Organization (WHO) as "Diffuse midline glioma, H3 K27M-mutant" (6).

In recent years, the recognition that surgical biopsy of brainstem tumors can be performed safely has led to a far more detailed understanding of the biology of DMGs, and has prompted the development of therapies directed against tumor-specific alterations (7, 8). However, the sensitive anatomic location of these tumors and the need for specialized surgical expertise has limited the broader adoption of surgical biopsy, especially at the time of recurrence. Hence, MR imaging and clinical examination are currently widely used to diagnose, and assess response to therapy, although both of these methods are limited in sensitivity and specificity (9–11). The inability to accurately assess disease response and treatment-related molecular changes confer significant challenges, particularly for emerging biologically targeted strategies such as immunotherapy (12, 13). Appropriate selection of tumor-specific treatment plans will require the ability to frequently monitor both the burden of disease and the ongoing genetic changes that clearly occur in these tumors over time.

The use of ctDNA to monitor disease progression is a non/minimally invasive method that has been increasingly used for disease monitoring in adult cancers including glioblastoma multiforme (GBM), melanoma, lung, breast, and colon cancers (14–18); however, such studies have not been applied to the pediatric population. Thus, there is an urgent need for the development of ctDNA assays for clinical applications in pediatric CNS patients.

Digital droplet PCR (ddPCR) is one of the most sensitive methods for detection and quantification of ctDNA when compared with Sanger sequencing, quantitative PCR, and next-generation sequencing platforms (19). The high sensitivity of ddPCR is attributed to the fact that PCR reactions are performed in millions of isolated droplets, allowing for detection of rare, low mutation allelic frequencies (19, 20). While Sanger sequencing of *H3F3A* p.K27M mutation in CSF of patients with DIPG was shown to be feasible (21), such an approach does not allow for calculating mutation allelic frequencies, and lacks sensitivity for

clinical applications. As the histone 3 K27M mutation is present at low mutant allelic frequencies, where one mutant allele exists among 30 alleles encoding isoforms of H3, a more sensitive approach is needed for detection of driver mutations in these tumors (22, 23). Therefore, the goal of this study was to assess the feasibility of detecting histone 3 K27M (H3K27M) and other driver mutations in CSF and plasma, as well as to investigate the clinical utility of tracking H3K27M in plasma ctDNA for disease monitoring. By using plasma collected longitudinally through an ongoing clinical trial (PNOC003; NCT02274987) conducted by the Pacific Pediatric Neuro-Oncology Consortium (PNOC), we were also able to correlate ctDNA levels with treatment response and progression.

### Materials and Methods

#### Biological specimens

All patient samples were collected after written informed consent was obtained by each patient or each patient's guardian for participation in a clinical trial, or biorepository as approved by the respective Institutional Review Boards of the University of California San Francisco (San Francisco, CA; IRB #14-13895), University of California San Diego (San Diego, CA; IRB #150450), and Children's National Health System (IRB #1339, #747). All studies involving human subjects were conducted in accordance with the U.S. Common Rule. CSF and cyst fluid were collected from patients with DMG consented to the Children's National (CN) brain tumor biorepository, while plasma was collected from patients with DIPG enrolled in the PNOC003 (NCT02274987) precision therapy clinical trial. This prospective I/II multi-institutional clinical trial (PNOC003, NCT02274987) led by PNOC enrolled newly diagnosed patients with DIPG to evaluate the feasibility of tumor genomic profiling of biopsies, and treated patients with precision therapy of up to four FDA-approved therapeutic agents (24). Blood was collected from enrolled patients for ctDNA analysis at the time of initial diagnosis, as well as with each subsequent MRI.

Whole blood was collected in a purple top potassium EDTA tube for isolation of plasma. The tube was then inverted to mix with the anticoagulant and spun at  $2,000 \times g$  for 15 minutes at  $4^{\circ}\text{C}$ . Blood was separated into three layers: plasma in the supernatant, white blood cell layer located between the plasma, and red blood cell pellet. Plasma was aliquoted and stored at  $-80^{\circ}\text{C}$  for future analyses.

Cerebrospinal fluid (CSF) was collected from subjects and processed according to the Children's National (CN) brain tumor biorepository standardized protocol. Briefly, CSF was spun at  $10,000 \times g$  for 10 minutes to eliminate cellular debris and supernatants were collected, aliquoted, and frozen at  $-80^{\circ}\text{C}$  for future analyses. Data for CSF and plasma samples collected from healthy pediatric and non-CNS malignant control pediatric subjects is shown in Supplementary Table S1. Time points for all CSF and plasma samples collected from subjects in this study is indicated in Supplementary Table S2.

#### DNA extractions

Genomic DNA was extracted from frozen tumor tissue using the Gentra Puregene kit (Qiagen). ctDNA was extracted from 1 mL of frozen plasma, 500  $\mu\text{L}$  of frozen CSF, and 200  $\mu\text{L}$  of frozen cyst fluid using the QIAamp circulating nucleic acids kit (Qiagen) according to the manufacturer's instructions. The ctDNA was subjected to preamplification prior to ddPCR using Q5 hot start

high-fidelity master mix (New England Biolabs), and 50 nmol/L each of forward and reverse primers for each gene as shown in Supplementary Table S3. Preamplification was performed in an ABI 2720 thermocycler at 98°C for 3 minutes, and nine cycles of 98°C for 10 seconds, at annealing temperature for 3 minutes, 72°C for 30 seconds, and an extension of 72°C for 2 minutes. The preamplified product was diluted 1:5 with TE buffer, pH 8.0.

#### ddPCR

All ddPCR reactions were conducted on the RainDrop ddPCR system according to the manufacturer's instructions. The ddPCR reaction was conducted with 1 × TaqMan Genotyping Mastermix (Life Technologies), 1 × RainDance droplet stabilizer, 12 μL of the diluted preamplified PCR product, 900 nmol/L of the forward and reverse primers, and 200 nmol/L of the mutant and wild-type probes (Supplementary Table S3). The prepared PCR reactions were added to the eight wells in a Source microfluidics chip, which is loaded along with an empty strip of PCR tubes onto the RainDrop Source machine. The RainDrop Source generates millions of droplets by using the components of the PCR reaction and surfactant containing fluorocarbon oil. The dropletized samples are dispensed into the PCR strip and used for the PCR reaction in the second step. PCR reactions were performed in an ABI 2720 thermocycler using the optimized conditions for each primer and probe sets. The amplified products in each droplet were detected using the RainDrop Sense machine and the Sense microfluidics chip based on the fluorescence signal emitted by the wild-type and mutant probes. The raw spectral data were analyzed using the RainDrop Analyst software to plot the signal for mutant and wild-type alleles. In the analysis software, the calculated matrix function was used to apply spectral compensation on intact droplets. Negative, wild-type, and mutant gates were applied on the basis of the no template negative, and genomic DNA-positive controls. All results were manually reviewed for false positives of the mutant alleles and background noise based on the no template negative control. Mutant allele frequency (MAF) was calculated by the percentage of mutant droplets divided by the sum of mutant and wild-type droplets.

#### MR Imaging

MR imaging of the brain was performed for all the patients according to the clinical protocol on either 1.5T or 3T scanners. Contrast-enhanced, FLAIR (fluid-attenuated inversion recovery), and T2-weighted images were used to measure tumor size. Anterior-posterior, transverse, and cranio-caudal dimensions were measured in mm on either PACS (Agfa Healthcare) or Horos (Horos Version 3.0) software packages. Tumor growth on MRI was defined as >25% increase in tumor volume-related FLAIR signal abnormality and/or development of new enhancing or nonenhancing lesions by an experienced neuro-oncologist (S.N. Magge) and neuroradiology fellow (M.S. Aboian) with guidance from a board-certified neuroradiologist (S. Cha).

#### Statistical analysis

Plasma ctDNA serial assessments and central MRI tumor measurement analyses were conducted independently in a blinded manner. Temporal plasma ctDNA MAFs were associated to clinical outcomes, and MRI tumor volume measurements at the end of the study. None of the MAF values collected were normally distributed; therefore all analyses used nonparametric tests. All data points for plasma and CSF represent technical triplicates and

duplicates, respectively. Error bars in all figures represent SEM. Paired samples were analyzed by a Wilcoxon signed-rank test, and unpaired values were analyzed by a Mann-Whitney test to obtain *P* values. A Kappa coefficient test was used to assess for agreement between plasma ctDNA and MRI evaluation of tumor response to radiotherapy. We assessed for at least a 50% reduction of H3K27M MAF in plasma ctDNA, in agreement with at least a 10% decrease in MRI tumor volume measurements at postradiation compared with baseline (*n* = 12). For all analyses, a significance threshold of 0.05 was used to define statistical significance.

## Results

### A sensitive and specific platform for discriminating rare, tumor-associated circulating DNA

Clinicopathologic and genomic characteristics of the tumors of our pediatric DMG patient cohort are shown in Fig. 1A. As expected, patients with DMGs harbored a predictable combination of mutations: 94% harbored histone 3 mutations (79% with H3.3K27M, 15% with H3.1K27M), and 6% were H3 wild-type. Our initial goal was to develop and validate a clinically relevant and minimally invasive liquid biopsy platform suitable for detection and quantification of somatic mutations associated with pediatric DMGs. To accomplish this goal, we validated our ddPCR probes for assessing mutation burden by using tumor genomic DNA from patients with DMG harboring oncohistone *H3F3A* (p.K27M), *HIST1H3B* (p.K27M), and partner mutants in genes *ACVR1* (p.G328V, p.R206H), *PPM1D* (p.E525X), *PIK3R1* (p.K567E), and *BRAF* (p.V600E; Supplementary Fig. S1A). In addition, no mutant clusters were observed where control brain genomic DNA was used as template (Supplementary Fig. S1A). To assess the sensitivity, we used a range (2.5 ng, 250 pg, 25 pg, and 2.5 pg) of genomic DNA as template for ddPCR and detected a corresponding linear decrease (10-fold) in MAF, indicating a low (2.5 pg) amount of DNA to be suitable for detection by ddPCR (Supplementary Fig. S1B).

To assess the specificity of our platform, we used a large control cohort of specimens from pediatric non-CNS malignant tumors (CSF = 16; plasma = 20) and probed for wild-type and mutant histone ctDNA. Our data demonstrated that any allelic frequency detected as equal or below 0.001% to be false positive in the case of histone p.K27M analysis (Supplementary Table S1). We also analyzed genomic DNA, CSF, and plasma obtained from three patients with DIPG who did not harbor histone three p.K27M mutations. As expected, histone-mutant copies were not detected in any of the specimen tested indicating the specificity of our platform (Supplementary Fig. S1C).

### CSF and plasma harbor ctDNA indicative of driver mutations associated with pediatric DMGs

Liquid biome specimens were analyzed from 84 subjects (48 DMG patients, and 36 patients with non-CNS disease), who were either consented for the Children's National (CN) brain tumor biorepository, or enrolled on an ongoing clinical trial PNOC003 (NCT02274987; Fig. 1B). A cohort of 110 biofluid samples (30 CSF, 79 plasma, and one cyst fluid) representing 48 DMG patients was processed for liquid profiling. CSF samples were collected at a single time point through the CN biorepository either at pretreatment, during therapy, or at postmortem from 27 patients with DMG, while serial sampling at pretreatment and postmortem was available for one patient with DIPG. Plasma specimens were

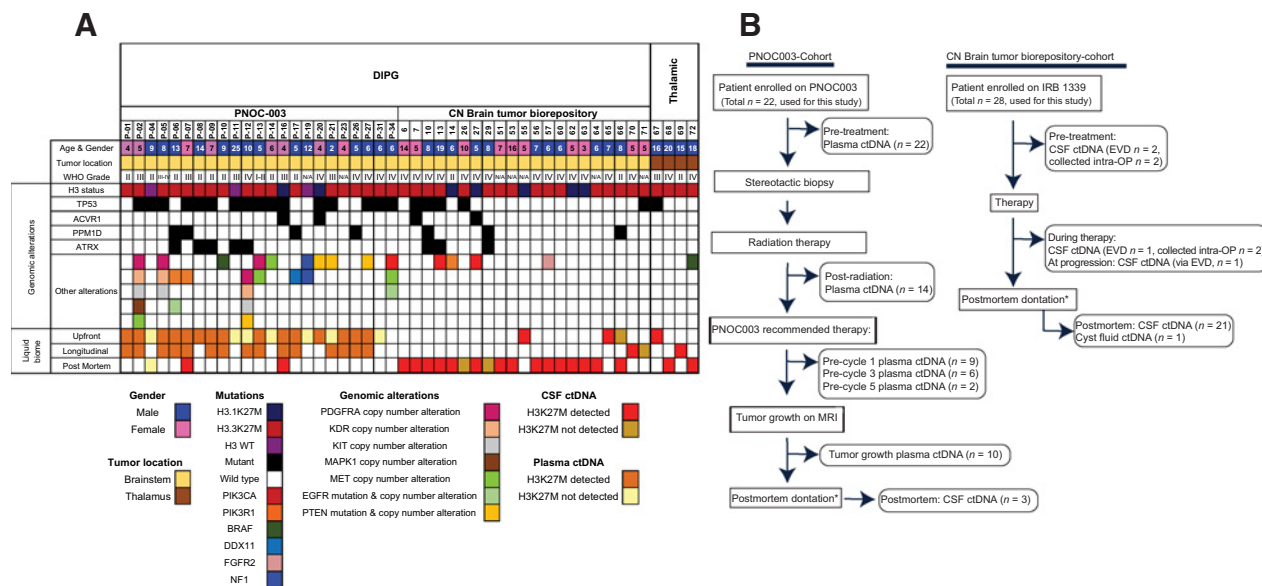


**Figure 1.**

Overview of biofluid specimens utilized in this study for detection of ctDNA in patients with diffuse midline glioma (DMG). **A**, Demographic, clinical, and molecular information for all patients analyzed in this study. Genomic alterations were obtained by tumor-sequencing data generated for PNOC003 trial, biorepository sequencing project, or other clinical studies. **B**, Flow chart portraying biofluid samples analyzed in this study. Patients were either enrolled in PNOC003 trial (DIPG) or Children's National (CN) brain tumor biorepository (DMG); \*, patients enrolled on IRB 1339 to donate specimens at postmortem.

obtained starting at diagnosis, and longitudinally throughout treatment from patients with DIPG enrolled in PNOC003 (NCT02274987; at initial biopsy  $n = 22$ , during treatment  $n = 15$ ; Fig. 1B; Supplementary Table S2). Three of the DIPG patients enrolled in PNOC003 also consented for CSF collection at postmortem via the CN biorepository, among which, two patients harbored H3 K27M and one was H3 wild-type (Fig. 1).

A total of 28 CSF samples were analyzed, where we successfully detected histone 3 mutant and wild-type alleles in 75% of CSF specimens collected at diagnosis, 67% of those collected during treatment, and 90% of those collected at postmortem (Fig. 2A). Tumor genome data were available for 24 of these subjects identifying one as histone 3 wild-type, and 23 as H3 K27M mutants. The histone 3 mutation status of four tumor samples was not known. Our analysis of CSF specimens validated the histone 3 wild-type specimen, as well as 20 of the 23 (87%) as H3 K27M-mutant subjects. The four samples for which tumor genome data were not available, were shown to be H3K27M mutant by ddPCR analysis of CSF.

We have previously shown that in addition to oncohistone mutations, DMGs harbor obligate partner mutations in genes such as *ACVR1*, *TP53*, *PPM1D*, and *PIK3R1* (25). We thus sought to determine whether biofluids represent a source for detection of multiple mutations for a particular patient. We first used tumor DNA known to harbor oncohistone and partner mutations (*ACVR1* p.R206H, *PIK3R1* p.K567E, or *BRAF* p.V600E) to optimize the experimental and analytical approach for multiplexed assays (Fig. 2b). We tested CSF obtained from these patients and showed the feasibility of detecting mutant and wild-type alleles, for oncohistone and obligate partners in *ACVR1*, *PIK3R1*, or *BRAF* (Fig. 2B).

We then assessed the effect of CSF location on ctDNA abundance. CSF collected from lateral ventricles, lumbar spine, cervical

spine, subdural (at biopsy), ventriculoperitoneal (VP) shunt, and the fourth ventricle (cisternae magna tap) was analyzed by ddPCR. CSF collected from the lateral ventricles was considered adjacent for thalamic tumors, while CSF collected from the fourth ventricle, and subdural space near brainstem during biopsy were considered adjacent locations for DIPGs. We detected a significantly higher MAF in CSF collected from adjacent locations for DIPGs. This was confirmed by our cohort based, and matched analysis of CSF collected from patients diagnosed with DIPG (Fig. 2D and E). Nonetheless, we report successful detection of H3 K27M ctDNA in all locations tested.

We previously reported the suitability of cyst fluid for identification of tumor associated proteins (26). Here, we analyzed tumor cyst fluid, CSF, and tumor genomic DNA obtained at postmortem from a patient diagnosed with DIPG. We showed that the cyst fluid is highly enriched for tumor DNA as suggested by the high number of histone-mutant DNA copies (Supplementary Fig. S2).

To assess the enrichment of ctDNA in CSF versus plasma, we tested these two biofluids and found a significantly higher allelic frequency of ctDNA in CSF ( $n = 27$  patients, 29 specimens) compared with plasma ( $n = 20$  subjects, 77 specimens;  $P < 0.0001$ ; Fig. 3A). We used matched CSF-plasma specimens ( $n = 2$  subjects) and found an enrichment of ctDNA in CSF compared with plasma within the same patient (Fig. 3b). We successfully detected H3K27M ctDNA in 87% (20/23 subjects) of CSF samples and 90% (18/20 subjects) of plasma samples analyzed from patients known to harbor oncohistones in their primary tumors. Although detectable, the levels of ctDNA in plasma were low, possibly due to challenges of overcoming the blood-brain barrier (BBB). Our data indicate that both CSF and plasma are a suitable source for detection of ctDNA, and

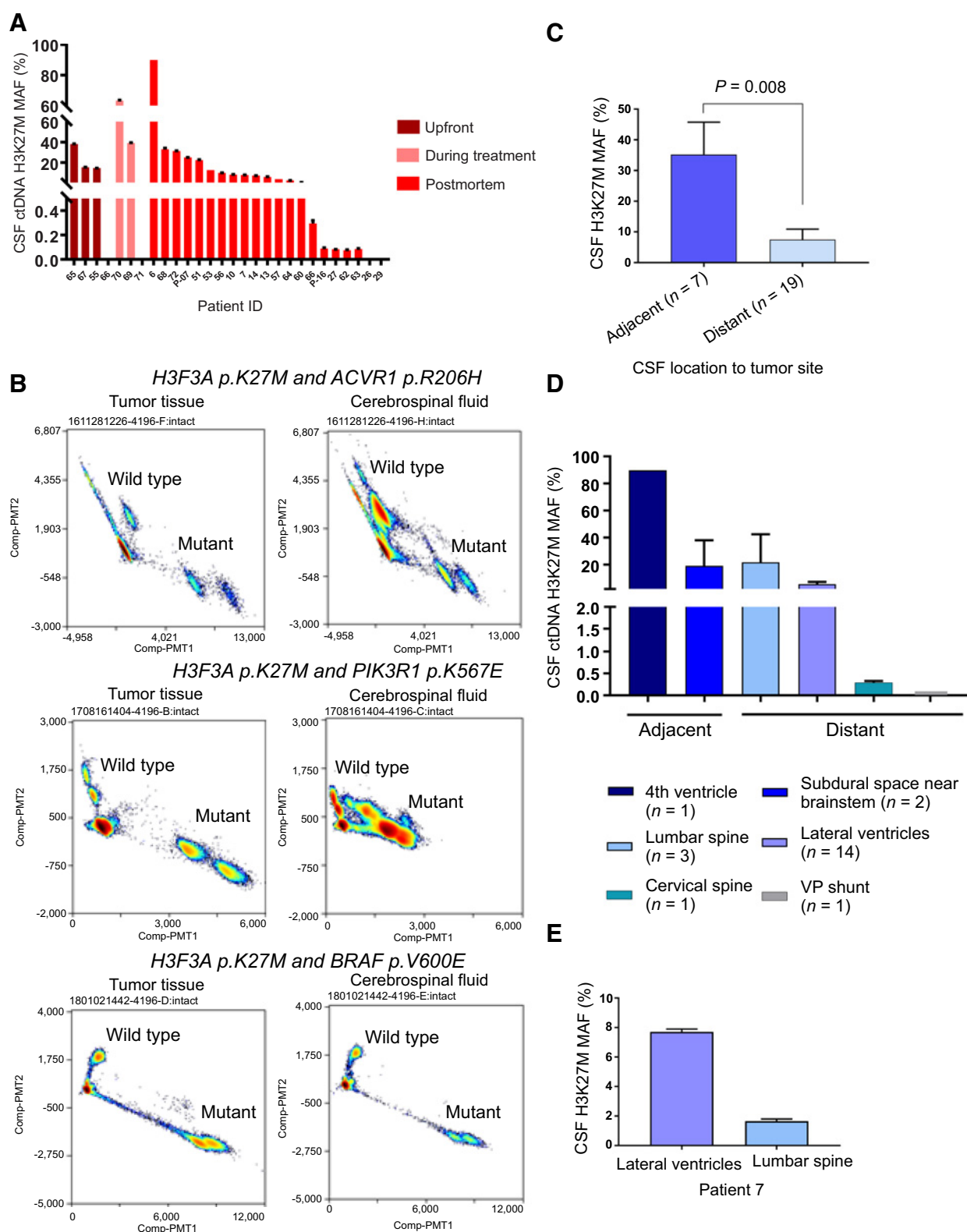


**Figure 2.** Detection of histone 3 p.K27M mutant (H3K27M) ctDNA in CSF of patients diagnosed with DMG. **A**, Detection of H3K27M ctDNA in CSF collected throughout disease. **B**, Multiplexed detection of major driver mutations in tumor and matched CSF. **C**, CSF collected from adjacent neuroanatomical locations yield a significantly (Mann-Whitney *U* test) higher H3K27M mutation allelic frequency in patients with DMG. Cohort based (**D**) and matched inpatient analysis (**E**) indicating higher H3K27M MAF levels in CSF from adjacent locations in patients with DIPG.

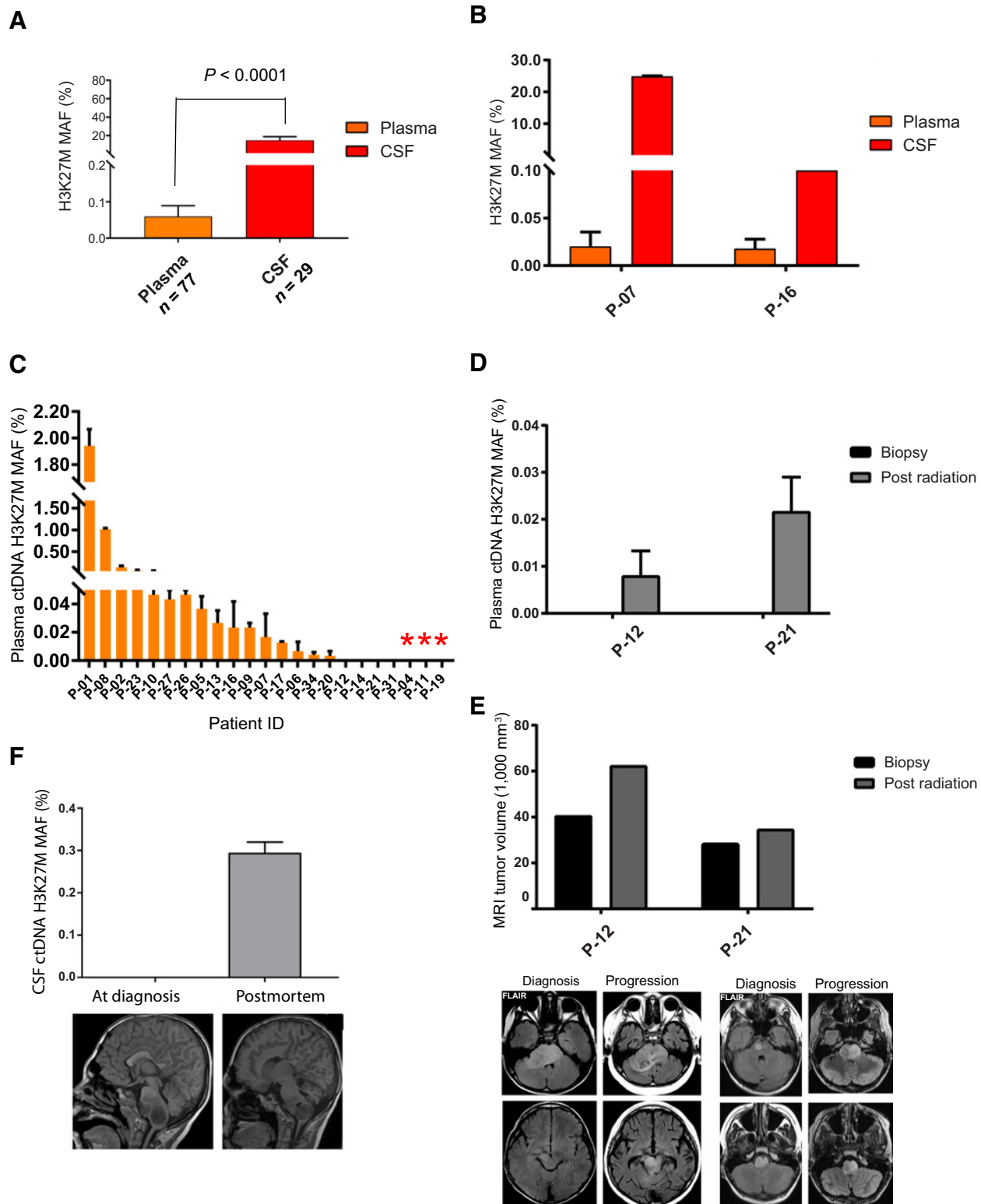


**Figure 3.** Abundance of histone 3 p.K27M mutation (H3K27M) ctDNA in biofluids of patients diagnosed with DMG. **A**, Significantly higher ctDNA MAFs for H3K27M were detected in CSF compared with plasma (Mann-Whitney *U* test). **B**, Higher H3K27M MAFs were present in CSF compared with plasma in the same patient. **C**, Plasma ctDNA collected at diagnosis in patients with DIPG enrolled in the PNO003 clinical trial analyzed for H3K27M. Red asterisk denotes histone 3 wild-type DIPGs. **D**, Detection of H3K27M plasma ctDNA at postradiation in two patients that lacked detection at diagnosis. **E**, Increase in tumor size by MRI at postradiation compared with diagnosis in patients shown in **D**. **F**, Detection of H3K27M ctDNA in CSF collected at postmortem that lacked detection at diagnosis, in a patient known to harbor H3.3 K27M in tumor.

Downloaded from <http://aacrjournals.org/clinccancerres/article-pdf/24/23/5850/2050411/5850.pdf> by guest on 06 November 2024

identification of tumor-associated somatic mutations. These results emphasize the potential value of liquid biopsy for complementing standard surgical biopsies, and the need for a highly sensitive platform for the detection of ctDNA in biofluids from patients with DMG.

#### Treatment response assessment using ctDNA quantification

To investigate the clinical translation of our approach, we studied plasma obtained from subjects diagnosed with DIPG who enrolled in the ongoing clinical trial (PNOC003). Analysis of upfront and serial plasma samples probing for histone mutations (H3.3 and H3.1) indicated the following: (i) histone mutations were successfully detected at diagnosis in 80% ( $n = 16$  of 20) of subjects harboring known histone mutations determined by genomic analysis of pretreatment biopsies (Fig. 3C); (ii) histone mutation was not detected at diagnosis in 20% of subjects with histone mutations ( $n = 4$  of 20), (iii) however, among these four subjects, histone mutation was subsequently detected following radiotherapy in two subjects where serial samples were available (Fig. 3D). MR image analysis of the two subjects for whom H3K27M ctDNA was absent at diagnosis, but present following radiotherapy indicated an increase in tumor volume following radiation (patient 12: 40.6 mm<sup>3</sup> to 62.4 mm<sup>3</sup>, and patient 21: 28.6 mm<sup>3</sup> to 34.8 mm<sup>3</sup>; Fig. 3E) suggesting that changes in tumor architecture in response to radiation, or temporary disruption of the BBB may contribute to the availability of ctDNA in plasma at different time points. Similarly, our analysis of serially collected CSF from a subject with H3 K27M DIPG at pretreatment and at postmortem, revealed an increase in ctDNA abundance at the later stage of disease (Fig. 3F).

To assess whether ctDNA can be developed as a surrogate biomarker of treatment response, we assessed the longitudinal plasma samples obtained from enrolled subjects (PNOC003). Overall, we found that subjects with DIPG had a decrease in ctDNA following radiotherapy. These findings were comparable with changes in MRI tumor volume measurements, where a significant decrease was observed in tumor burden following radiotherapy as determined by a paired Wilcoxon signed-rank analysis ( $n = 14$ ; Fig. 4A). We report an agreement of 75% between ctDNA response (at least 50% decrease) and MRI tumor volume measurements (at least 10% decrease) at postirradiation compared with baseline using the Kappa coefficient analysis ( $n = 12$  subjects, kappa = 0.4,  $P = 0.078$ ).

We subsequently analyzed only the subjects who followed the recommended precision therapy ( $n = 9$ ), and found a decrease in plasma ctDNA from biopsy to early cycles of precision therapy (pre-C1). Moreover, 60% (3/5) of patients showed an increase in plasma ctDNA at progression, suggesting that plasma ctDNA may agree with detecting tumor growth (Fig. 4B). The longitudinal changes in H3 K27M from biopsy to posttherapy closely mirrored the trend of MRI-based clinical response in these subjects, characterized by a steady decrease following radiation and chemotherapy, and an increase at progression (Fig. 4C). Among subjects that followed PNOC003 recommended therapy, pre-C3 was the time point with the highest sample availability for ctDNA analysis and radiographic evaluation. We found a decrease in plasma ctDNA congruent with the diminished tumor burden measured by MRI (Fig. 4D). Nonetheless, these findings infer the clinical utility of plasma ctDNA for monitoring response, comparable with MRI evaluation. These findings were further evaluated in one patient with DIPG who followed recommended therapy, where

our analysis displayed that changes in ctDNA MAFs during the course of disease precisely reflected tumor response. Following enrollment in a different clinical trial, we detected a decrease in plasma ctDNA, indicative of a response to therapy (Fig. 4e). Notably, patient-specific temporal analysis of changes in MAF of histone 3 mutation indicated a close agreement of ctDNA level with both clinical course of the disease, and tumor response, as revealed by MR imaging volumetric analysis (P-02, P-10, P-13, P-27). In some patients (P-01, P-23), ctDNA levels showed fluctuations when compared with MRI assessment. This may be due to the limited sensitivity of MRI in detecting small variations in tumor size which needs further validation in a larger cohort (Supplementary Fig. S3).

We then assessed whether an increase in H3 K27M ctDNA accompanied tumor spread as determined by MRI, molecular, and/or histologic studies. Tumor extension was determined by MRI obtained during the course of the treatment, or molecular and histopathologic review of autopsied brain specimens. Tumor involvement beyond pons for patients enrolled in the clinical trial (PNOC003) was determined by central MRI review at diagnosis, during therapy, or at tumor growth. We found that increased levels of CSF ctDNA corresponded to tumor spread; however, the small sample size for the availability of CSF for DIPGs with tumor dissemination precluded statistical significance. On the contrary, plasma collected at various times throughout disease (diagnosis, during treatment, or at tumor growth) was not predictive or indicative of tumor spread beyond pons (Supplementary Fig. S4).

## Discussion

Outcomes for children diagnosed with DMG have not changed despite decades of clinical research. Recent advancements in genomic, epigenomic, and proteomic profiling provide new opportunities for accelerating development of novel therapeutic interventions for patients with these tumors. Collection of post-mortem specimens led to the identification of oncohistones as driver mutations as well as other partner mutations, and newer clinical trials are building upon this knowledge to identify rational, biologically targeted treatment approaches (4, 5, 25). However, the difficulty of performing repeated surgical biopsies in the pons is a barrier to the accurate assessment of responses to therapy.

Liquid biopsy has emerged as a useful tool for diagnosis, and measurement of efficacy in the treatment of adult cancers. ctDNA has been used to determine patient's mutation profiles, as a biomarker for molecular-based disease monitoring, and recurrence in adult chronic lymphocytic leukemia, breast, and colon cancer (14, 18, 27). The only reported liquid biopsy approach for pediatric DMGs was established using Sanger sequencing that does not allow for quantification of ctDNA (21). Here we report the establishment of a sensitive, specific, rapid, and minimally invasive methodology for tumor surveillance of pediatric DMGs by monitoring the liquid biome. Specifically, we show the detection of mutations associated with pediatric DMGs such as DIPG and thalamic tumors, using patients' CSF and plasma.

Given the paucity of tumor DNA in these rare cancers, and the invasive nature of surgical biopsy, the multiplexed mutation analysis we used allows for maximized clinical utility of a single accessible biofluid specimen. Necrotic biopsy tumor tissue may sometimes result in degraded nucleic acid content unsuitable for subsequent sequencing analyses; in such cases, if CSF or cyst fluid

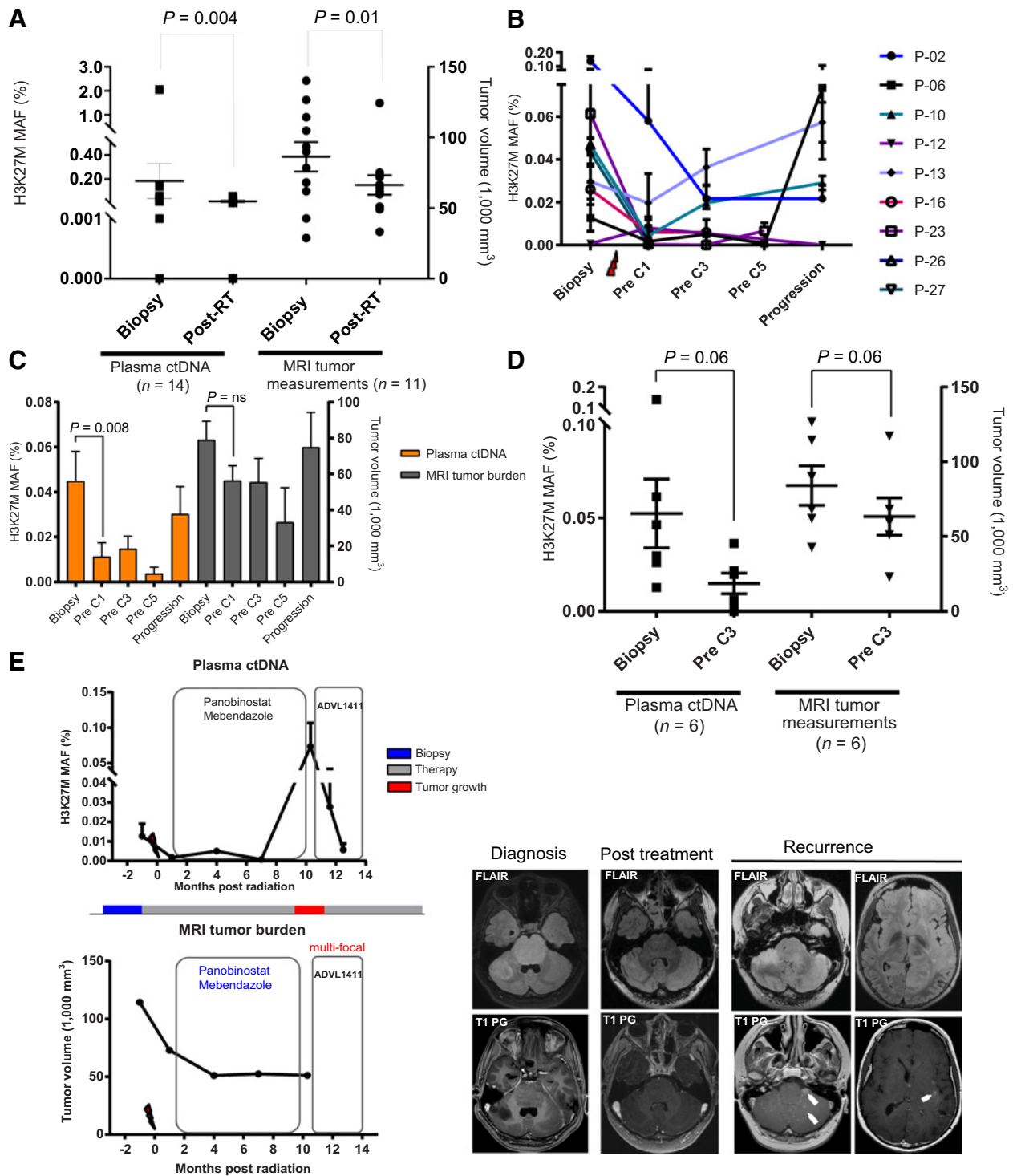


**Figure 4.** Temporal analysis of plasma ctDNA agrees with response to therapy in patients with DIPG. **A**, Significant decrease in plasma ctDNA and MRI tumor volumes in response to radiotherapy. **B**, Serial plasma ctDNA analysis for changes in H3K27M throughout course of treatment in patients that followed PNOCC03 recommended therapy. **C**, Fluctuations in plasma ctDNA and MRI tumor volumes in an average of nine patients (pre-C1) reflect similar trends posttherapy, and at progression. **D**, Decrease in plasma ctDNA and MRI tumor burden from diagnosis to pre-cycle 3 of PNOCC03 recommended therapy. **E**, Dynamic changes in plasma ctDNA and MRI tumor measurements in patient P-06 in response to therapy. FLAIR and T1-weighted post-gadolinium MR images prior to treatment demonstrating prominent expansile pontine mass and an additional focus within right cerebellar hemisphere that demonstrates evidence of enhancement. After treatment, the pontine and right cerebellar hemisphere lesions decreased in size. Paired Wilcoxon signed-rank tests were used to derive all *P* values.

Downloaded from <http://aacrjournals.org/clinccancerres/article-pdf/24/23/5850/2050411/5850.pdf> by guest on 06 November 2024



is available, these may serve as more adequate materials for sequencing. CSF collected for clinical purposes may serve as a surrogate for detecting tumor driver mutations. Indeed, in many cases an extra-ventricular drain is placed to relieve pressure prior to any surgical interventions. In such cases, our platform will allow for detecting tumor-associated mutations in the advance of any surgical interventions.

We have shown that tumor-associated ctDNA can be quantified using ddPCR, which will allow for a rapid and more sensitive method for surveying tumor mutations. This represents a key advance particularly for tumors with limited tissue acquisition, or prohibitive sampling at multiple time points. Many of the ongoing trials have exclusion and inclusion criteria that are based on patient's cancer mutation profile. For example, newly launched clinical trials, including an immunotherapy trial will enroll only patients with pediatric glioma who harbor the H3K27M mutation (NCT03416530, NCT02960230) and therefore establishing non-invasive tools for the detection of mutations, such a ctDNA, is critical.

Using plasma collected through the ongoing clinical trial (PNOC003), we show that MAF is readily obtained from ctDNA present in liquid biome, and that MAF might correlate with treatment response. Our report is the first to provide an indication of the potential utility of ctDNA for tumor profiling, and assessment of tumor response to therapy in pediatric patients with DMGs. These results indicate the feasibility of incorporating liquid biopsy as a sensitive and minimally invasive tool to inform clinical management for children with DMGs.

While we report the detection of ctDNA in both CSF and plasma, the exact mechanism of tumor DNA release into the biofluid is not well understood. A survey of published manuscripts indicated that ctDNA is released from multiple sources, including living cells, apoptotic and/or necrotic tumor cells (19, 28–30). We also found that CSF yielded a significantly higher amount of ctDNA compared with plasma. This is most likely due to the location of biofluids in relation to site of tumor, and challenges of overcoming the BBB for release of ctDNA into plasma.

Our lack of detection of ctDNA in plasma obtained at biopsy from four subjects (H3 mutant by biopsy) may suggest high BBB integrity and thus lack of ctDNA. Subsequent analyses detected ctDNA in plasma drawn for two of these four subjects following radiotherapy, indicating the potential role of radiotherapy for temporary disruption of the BBB. Moreover, as the cellular turnover in a growing tumor increases, apoptotic and necrotic tumor cells are hypothesized to contribute to the increased release of ctDNA into biofluids (29). As such, we expected to observe an initial rise in ctDNA as tumor cells die and release DNA into biofluids. However, our tested time points fell after the completion of radiotherapy when the tumor mass was reduced in most patients as assessed by MRI, corresponding to the expectant reduced number of ctDNA. An issue to be determined is whether inclusion of earlier collection time points during the course of radiotherapy, would allow us to detect an initial spike in ctDNA immediately after early radiation treatments, followed by stabilization of ctDNA at maximal tumor response. Our study suggests that collection of multiple plasma draws at diagnosis and during treatment will be more informative as ctDNA may not be detectable in initial blood draws.

We have recently shown that DIPG tumor cells disseminate throughout the brain during the course of disease (25, 31). Our ctDNA analysis in patients with DIPG was indicative of tumor

expansion beyond pons, where an increased amount of ctDNA in CSF was observed in patients who exhibited tumor spread; however, these findings were not replicated using ctDNA assessment in plasma. Studies of a larger cohort in clinical settings are required to assess the statistical significance of our finding.

More importantly, our results indicate the unique strength of liquid biopsy for assessing the molecular landscape of DMGs noninvasively, and potential for longitudinal assessment of tumor response to therapy, which is a new tool that is complementary to MR imaging. Similar to the clinical utility of ctDNA for monitoring response to therapy with respect to MRIs in adult GBMs (17), despite a small sample size, we found a significant reduction in ctDNA following radiotherapy. Similar patterns in temporal changes of ctDNA and MRI assessments of tumor response indicated that our ddPCR analysis of plasma is highly translational, and offers a novel platform for assessing tumor response, regression and/or progression in DMGs. Our liquid biopsy approach may also be expanded for facilitating diagnosis, longitudinal monitoring, and assessing recurrence in other childhood CNS cancers.

In summary, we have shown that CSF and plasma ctDNA analysis of children with DMG is feasible, shows promise for detecting mutational load, provides an additional means for molecular disease characterization, and most importantly is a clinically relevant and might serve as an additional method for assessing tumor response to treatment.

#### Disclosure of Potential Conflicts of Interest

No potential conflicts of interest were disclosed.

#### Authors' Contributions

**Conception and design:** E. Panditharatna, M. Kambhampati, J.R. Crawford, R.J. Packer, M. Prados, S. Mueller, J. Nazarian

**Development of methodology:** E. Panditharatna, S. Mueller

**Acquisition of data (provided animals, acquired and managed patients, provided facilities, etc.):** M. Kambhampati, S.N. Magge, N. Gupta, J.S. Myseros, E.I. Hwang, C. Kline, K.E. Warren, W.S. Liang, R.J. Packer, M. Prados, S. Mueller

**Analysis and interpretation of data (e.g., statistical analysis, biostatistics, computational analysis):** E. Panditharatna, L. Kilburn, M.S. Aboian, M. Kambhampati, H. Gordish-Dressman, E.I. Hwang, R.J. Packer, A.C. Resnick, S. Mueller, J. Nazarian

**Writing, review, and/or revision of the manuscript:** E. Panditharatna, L. Kilburn, M.S. Aboian, H. Gordish-Dressman, S.N. Magge, N. Gupta, J.S. Myseros, E.I. Hwang, C. Kline, J.R. Crawford, K.E. Warren, S. Cha, M.E. Berens, R.J. Packer, A.C. Resnick, M. Prados, S. Mueller, J. Nazarian

**Administrative, technical, or material support (i.e., reporting or organizing data, constructing databases):** E. Panditharatna, M. Kambhampati

**Study supervision:** C. Kline, J. Nazarian

#### Acknowledgments

The authors would like to acknowledge the generosity of all patients' and their families. We would also like to thank all staff members of Pediatric Pacific Neuro-Oncology Consortium (PNOC) for their support. Human tissue and CSF was obtained from University of Maryland Brain and Tissue Bank, which is a brain and tissue repository of the NIH NeuroBioBank. E. Panditharatna is a predoctoral student in the Molecular Medicine Program of the Institute for Biomedical Sciences at The George Washington University. This work is from a dissertation to be presented to the above program in partial fulfillment of the requirements for the PhD degree. This work was supported by funding from the V foundation (Atlanta, GA), Goldwin Foundation (St. Lincoln, NE), Pediatric Brain Tumor Foundation (Asheville, NC), Smashing Walnuts Foundation (Middleburg, VA), The Gabriella Miller Kids First Data Resource Center, Zickler Family Foundation (Chevy Chase, MD), Clinical and Translational Science Institute at Children's National (5UL1TR001876-03), Piedmont Community Foundation (Middleburg, VA), Musella Foundation (Hewlett, NY), Mathew Larson Foundation (Franklin Lake, NJ), The Lilabeau Foundation for Pediatric

Brain Cancer Research (Silver Spring, MD), Childhood Brain Tumor Foundation (Germantown, MD). M.S. Aboian was supported by NIH T32 grant (Bethesda, MD), and American Society of Neuroradiology (Oak Brook, IL).

The costs of publication of this article were defrayed in part by the payment of page charges. This article must therefore be hereby marked

*advertisement* in accordance with 18 U.S.C. Section 1734 solely to indicate this fact.

Received May 4, 2018; revised June 27, 2018; accepted August 30, 2018; published first October 15, 2018.

## References

- Ostrom QT, Gittleman H, de Blank PM, Finlay JL, Gurney JG, McKean-Cowdin R, et al. American Brain Tumor Association Adolescent and Young Adult Primary Brain and Central Nervous System Tumors Diagnosed in the United States in 2008-2012. *Neuro-oncol* 2016;18:i1-i50.
- Castel D, Philippe C, Calmon R, Le Dret L, Truffaux N, Boddaert N, et al. Histone H3F3A and HIST1H3B K27M mutations define two subgroups of diffuse intrinsic pontine gliomas with different prognosis and phenotypes. *Acta Neuropathol* 2015;130:815-27.
- Mackay A, Burford A, Carvalho D, Izquierdo E, Fazal-Salom J, Taylor KR, et al. Integrated molecular meta-analysis of 1,000 pediatric high-grade and diffuse intrinsic pontine glioma. *Cancer Cell* 2017;32:520-37 e5.
- Schwartzentruber J, Korshunov A, Liu XY, Jones DT, Pfaff E, Jacob K, et al. Driver mutations in histone H3.3 and chromatin remodelling genes in paediatric glioblastoma. *Nature* 2012;482:226-31.
- Wu G, Broniscer A, McEachron TA, Lu C, Paugh BS, Beckwith J, et al. Somatic histone H3 alterations in pediatric diffuse intrinsic pontine gliomas and non-brainstem glioblastomas. *Nat Genet* 2012;44:251-3.
- Louis DN, Perry A, Reifenberger G, von Deimling A, Figarella-Branger D, Cavenee WK, et al. The 2016 World Health Organization Classification of Tumors of the Central Nervous System: a summary. *Acta Neuropathol* 2016;131:803-20.
- Plessier A, Le Dret L, Varlet P, Beccaria K, Lacombe J, Meriaux S, et al. New in vivo avatars of diffuse intrinsic pontine gliomas (DIPG) from stereotactic biopsies performed at diagnosis. *Oncotarget* 2017;8:52543-59.
- Carai A, Mastronuzzi A, De Benedictis A, Messina R, Cacchione A, Miele E, et al. Robot-assisted stereotactic biopsy of diffuse intrinsic pontine glioma: a single-center experience. *World Neurosurg* 2017;101:584-8.
- Hargrave D, Chuang N, Bouffet E. Conventional MRI cannot predict survival in childhood diffuse intrinsic pontine glioma. *J Neurooncol* 2008; 86:313-9.
- Laprie A, Pirzkall A, Haas-Kogan DA, Cha S, Banerjee A, Le TP, et al. Longitudinal multivoxel MR spectroscopy study of pediatric diffuse brainstem gliomas treated with radiotherapy. *Int J Radiat Oncol Biol Phys* 2005; 62:20-31.
- Riley GT, Armitage PA, Batty R, Griffiths PD, Lee V, McMullan J, et al. Diffuse intrinsic pontine glioma: is MRI surveillance improved by region of interest volumetry? *Pediatr Radiol* 2015;45:203-10.
- Chheda ZS, Kohanbash G, Okada K, Jahan N, Sidney J, Pecoraro M, et al. Novel and shared neoantigen derived from histone 3 variant H3.3K27M mutation for glioma T cell therapy. *J Exp Med* 2018;215:141-57.
- Ochs K, Ott M, Bunse T, Sahn F, Bunse L, Deumelandt K, et al. K27M-mutant histone-3 as a novel target for glioma immunotherapy. *Oncoimmunology* 2017;6:e1328340.
- Tie J, Wang Y, Tomasetti C, Li L, Springer S, Kinde I, et al. Circulating tumor DNA analysis detects minimal residual disease and predicts recurrence in patients with stage II colon cancer. *Sci Transl Med* 2016;8:346a92.
- Tsao SC, Weiss J, Hudson C, Christophi C, Cebon J, Behren A, et al. Monitoring response to therapy in melanoma by quantifying circulating tumour DNA with droplet digital PCR for BRAF and NRAS mutations. *Sci Rep* 2015;5:11198.
- Garcia-Murillas I, Schiavon G, Weigelt B, Ng C, Hrebien S, Cutts RJ, et al. Mutation tracking in circulating tumor DNA predicts relapse in early breast cancer. *Sci Transl Med* 2015;7:302ra133.
- De Mattos-Arruda L, Mayor R, Ng CK, Weigelt B, Martinez-Ricarte F, Torrejon D, et al. Cerebrospinal fluid-derived circulating tumour DNA better represents the genomic alterations of brain tumours than plasma. *Nat Commun* 2015;6:8839.
- Schiavon G, Hrebien S, Garcia-Murillas I, Cutts RJ, Pearson A, Tarazona N, et al. Analysis of ESR1 mutation in circulating tumor DNA demonstrates evolution during therapy for metastatic breast cancer. *Sci Transl Med* 2015;7:313ra182.
- Diaz LA Jr, Bardelli A. Liquid biopsies: genotyping circulating tumor DNA. *J Clin Oncol* 2014;32:579-86.
- Wang W, Song Z, Zhang Y. A Comparison of ddPCR and ARMS for detecting EGFR T790M status in ctDNA from advanced NSCLC patients with acquired EGFR-TKI resistance. *Cancer Med* 2017;6:154-62.
- Huang TY, Piuanti A, Lulla RR, Qi J, Horbinski CM, Tomita T, et al. Detection of Histone H3 mutations in cerebrospinal fluid-derived tumor DNA from children with diffuse midline glioma. *Acta Neuropathol Commun* 2017; 5:28.
- Bender S, Tang Y, Lindroth AM, Hovestadt V, Jones DT, Kool M, et al. Reduced H3K27me3 and DNA hypomethylation are major drivers of gene expression in K27M mutant pediatric high-grade gliomas. *Cancer Cell* 2013;24:660-72.
- Lewis PW, Muller MM, Koletsky MS, Cordero F, Lin S, Banaszynski LA, et al. Inhibition of PRC2 activity by a gain-of-function H3 mutation found in pediatric glioblastoma. *Science* 2013;340:857-61.
- Mueller S, Liang W, Gupta N, Magge S, Kilburn L, Crawford J, et al. DIPG-40. PNOC-003: precision medicine trial for children with diffuse intrinsic pontine glioma. *Neuro-oncol* 2017;19:iv14-iv.
- Nikbakht H, Panditharatna E, Mikael LG, Li R, Gayden T, Osmond M, et al. Spatial and temporal homogeneity of driver mutations in diffuse intrinsic pontine glioma. *Nat Commun* 2016;7:11185.
- Saratsis AM, Yadavilli S, Magge S, Rood BR, Perez J, Hill DA, et al. Insights into pediatric diffuse intrinsic pontine glioma through proteomic analysis of cerebrospinal fluid. *Neuro-oncol* 2012;14:547-60.
- Yeh P, Hunter T, Sinha D, Ftouni S, Wallach E, Jiang D, et al. Circulating tumour DNA reflects treatment response and clonal evolution in chronic lymphocytic leukaemia. *Nat Commun* 2017;8:14756.
- van der Vaart M, Pretorius PJ. Circulating DNA. Its origin and fluctuation. *Ann N Y Acad Sci* 2008;1137:18-26.
- Jahr S, Hentze H, Englisch S, Hardt D, Fackelmayer FO, Hesch RD, et al. DNA fragments in the blood plasma of cancer patients: quantitations and evidence for their origin from apoptotic and necrotic cells. *Cancer Res* 2001;61:1659-65.
- Stroun M, Lyautey J, Lederrey C, Olson-Sand A, Anker P. About the possible origin and mechanism of circulating DNA apoptosis and active DNA release. *Clin Chim Acta* 2001;313:139-42.
- Kambhampati M, Perez JP, Yadavilli S, Saratsis AM, Hill AD, Ho CY, et al. A standardized autopsy procurement allows for the comprehensive study of DIPG biology. *Oncotarget* 2015;6:12740-7.